Ouyang *et al. EURASIP Journal on Wireless Communications and Networking* (2019) 2019:247
https://doi.org/10.1186/s13638-019-1585-z

EURASIP Journal on Wireless Communications and Networking

RESEARCH Open Access

Optimal interference range for minimum Bayes risk in binomial and Poisson wireless networks

Min Ouyang, Wenxiao Shi*, Ruidong Zhang and Wei Liu

Abstract

Interference is the main performance-limiting factor in most wireless networks. Protocol interference model is extensively used in the design of wireless networks. However, the setting of interference range, a crucial part of the protocol interference model, is rather heuristic and remains an open problem. In this paper, we use the stochastic geometry and the direct approach to obtain the associated feasibility distributions. After that, we use the binary hypothesis testing to achieve the Bayes risk under binomial point process (BPP) and Poisson point process (PPP), respectively. According to the first derivative of the Bayes risk, we provide the equation to achieve the optimal interference range for minimum Bayes risk. We extend the method proposed by Wildman et al. to a more general situation. Furthermore, we show that for infinite PPP, those two methods converge to the same results. Several numerical results for wireless networks under BPP, finite PPP, and infinite PPP are given. Simulation results show that in the finite wireless network, the BPP method performs better than the PPP method.

Keywords: Bayes risk, Binary hypothesis testing, Interference range, Stochastic geometry, Wireless networks

1 Introduction

Interference range is a crucial part of the protocol interference model. Under the protocol interference model, the transmission between the reference receiver and the reference transmitter is successfully received, when there is no interference transmitter within the interference range of the reference receiver [1]. In the last two decades, interference range is widely used in wireless networks, such as ad hoc networks [2–5], wireless mesh networks [6–10], sensor networks [11, 12], cellular networks [13, 14], and WiMAX networks [15]. The setting of interference range has a large effect on the performance of wireless networks [10, 11, 16, 17]. In wireless networks based on the IEEE 802.11 standard, interference range is usually set to be twice as large as the transmission range [7, 8, 18, 19]. In CSMA-based wireless networks, the interference range is set equal to the carrier sensing range [4, 6, 9, 20]. Several works [2, 4, 21–23] set the interference range by restricting the signal-to-interference-and-noise ratio (SINR) to a threshold. In their works, only one interference transmitter is considered when calculating the SINR. The interference ranges in the mentioned literature are set without fully considering the effect of the networks. However, the optimal interference range may be a function of network parameters, and the casual setting of the interference range will depress the performance of wireless networks. The setting of the interference range is rather heuristic and remains an open problem [24].

Several works have further studied the setting of the interference range. Hasan and Andrews [25] study the optimal interference range (guard zone) to maximize transmission capacity in CDMA-based wireless ad hoc networks. Iyer et al. [26] study the minimum interference range under the additive interference model, the capture threshold model, and the interference range model, respectively. Zhou et al. [15] deduce the probability density of the ratio between the interference range and the one-hop distance. The randomness of the ratio is due to the random thermal noise. Besides, they only consider one interference transmitter. Shi et al. [24] discuss the bounds for the maximum interference range. They deduce the lower bound of the maximum interference range with

*Correspondence: swx@jlu.edu.cn
[1]College of Communication Engineering, Jilin University, Nanhu Road, 130012 Changchun, China

the maximum transmission range, and the upper bound with the maximum range that a band can be reused. Their work gives the span of maximum interference range. However, the exact value of the interference range remains unknown.

Zhang et al. [27] propose the physical-ratio-K (PRK) interference model as a reliability-oriented instantiation of the protocol model. Furthermore, they study the effect of K on the reliability and throughput. Hasan and Ali [28] present the optimal interference range (guard zone) expression that maximizes the density of successful transmissions under an outage constraint. Wildman and Weber [29] study the optimal interference range to minimize the Bayes risk of the protocol interference model in wireless Poisson networks. In [30], they also investigate the interference range to maximize the correlation of the physical interference model and protocol interference model in Poisson networks. The authors use the binary hypothesis testing to achieve the interference range for minimum Bayes risk. However, their works are only suitable for Poisson networks. The Poisson point process has two deficiencies when modeling finite networks. The first one is no consideration of the network boundary. The second one is the allowance of unbounded nodes in a finite area. The optimal interference range for finite network needs further study.

In this paper, our main contribution is proposing a method of setting the optimal interference range which is applicable for a more general situation. We employ the binary hypothesis testing framework to outline the relationship between the physical and protocol interference model. The optimal interference range is configured to minimize the Bayes risk of the protocol interference model.

The first contribution of this paper is proposing a method to achieve the optimal interference range for binomial wireless networks. We adopt the direct approach to obtain the associated feasibility distributions for wireless networks under BPP. Furthermore, we calculate Bayes risk with those distributions and deduce the optimal interference range to minimize the Bayes risk.

Next, we derive the optimal interference range for finite and infinite Poisson wireless networks. Furthermore, we demonstrate that the optimal interference range found by Wildman et al. [30] is the special case of the infinite PPP.

Finally, we present several numerical results of Bayes risks, receiver operating characteristic (ROC), and area under curve (AUC) under BPP, finite PPP, and infinite PPP. Our results reveal that the BPP method and the finite PPP method achieve smaller optimal interference range than the infinite PPP method. In the finite wireless network, the BPP method performs better than the PPP methods.

The rest of this paper is organized as follows. In Section 2, we introduce the wireless network model, including the propagation model, physical interference model, and protocol interference model. In Section 3, we introduce the binary hypothesis testing and Bayes risk. In Section 4, we provide the feasibility distributions under binomial wireless networks and Poisson wireless networks, respectively. In Section 5, we deduce the Bayes risk and optimal interference range. In Section 6, we give some numerical results for BPP and PPP. Section 7 concludes this paper. Finally, for clarity, long proofs are presented in the Appendix.

2 Network model

We consider a network, in a two-dimensional region A, with a reference receiver RX_0, a reference transmitter TX_0, and M interference transmitters $TX_1, \cdots, TX_M$. Assume that all interference transmitters are active and consist of a point process in a snapshot. In this paper, we concentrate on analyzing the performance (the Bayes risks) of the networks at a snapshot with stochastic geometry tool. For the analyzing of the long-term metrics, queuing theory should also be incorporated [31]. Without a loss of generality, due to the stationarity of the point process, we may take the reference receiver to be at the origin. The distance is normalized by the distance from TX_0 to RX_0, denoted by $d_0 = 1$. Let d_i denote the distance from TX_i to RX_0. The area of the network region is denoted by $|A|$. As the power allocation is not considered in this paper, we assume that all transmitter's power P_i for all $i \in \{0, \cdots, M\}$ is the same.

2.1 Propagation model

Our signal propagation model considers the path loss with Rayleigh fading. The signal received by RX_0 from TX_i, denoted by P_{Ri}, is

$$P_{Ri} = P_i h_i d_i^{-\alpha} \tag{1}$$

where h_i is the i.i.d. unit-mean exponential shadowing factor for all $i \in \{0, \cdots, M\}$, $\alpha > 2$ is the path loss exponent. The value of α is typically between 2 and 8 as in [32] and [33].

2.2 Physical interference model

Under physical interference model, transmission from TX_0 is successfully received by RX_0 if the SINR is no less than a defined SINR threshold β, which can be expressed as follows:

$$\mathrm{SINR} = \frac{h_0}{\mathrm{SNR}^{-1} + \sum_{i=1}^{M} h_i d_i^{-\alpha}} \geq \beta \tag{2}$$

where SNR is the average signal-to-noise ratio. The interference range is mainly affected by interference, and we mainly interest in the effect of interference in this paper. As wildly assumed in [25–34], we calculate the noise with the average. Remember that distance is normalized by d_0,

and the SNR^{-1} is achieved by dividing the transmitter power P_0 with the average noise.

Let random variables $H = \mathbf{1}\{\mathrm{SINR} \geq \beta\}$ represent the physical model feasibility, denoted by H_1, of the transmission from TX_0 to RX_0. The indicator $\mathbf{1}_A$ has the value 1 for all elements of A and the value of 0 for all elements not in A. The physical model failure is denoted by H_0.

2.3 Protocol interference model

Under protocol interference model, a transmission from TX_0 to RX_0 is successful, if there are no interference transmitters within the interference range of RX_0, denoted by R_I. Let random variables $D = \mathbf{1}\{d_i \geq R_I, \forall i \neq 0\}$ represent the protocol model feasibility, denoted by D_1, of the transmission from TX_0 to RX_0. The protocol model failure is denoted by D_0.

3 Binary hypothesis testing and Bayes risk

In wireless networks, the physical interference model is considered as a more realistic description of the effects of interference [35]. Appropriate setting of the interference range of the protocol interference model can maximize the similarity between the two models. The appropriate setting here means to set the interference range to be the optimal interference range which maximizes the similarity. In this paper, we employ the binary hypothesis testing framework in [36] to describe the relationship between the two models. The minimum Bayes risk maps the maximum similarity. The optimal interference range to maximize the similarity between the two models is equivalent to minimize the Bayes risk.

In the binary hypothesis testing, the two hypotheses (null hypothesis H_0 and alternate hypothesis H_1) represent the possible outcomes (failure and success) under the physical interference model. The two decisions (D_0 and D_1) represent the possible observations (failure and success) under the protocol interference model. For this binary hypothesis testing problem, four possible cases can occur:

(1) Decide D_0 when H_0 is true.
(2) Decide D_0 when H_1 is true.
(3) Decide D_1 when H_0 is true.
(4) Decide D_1 when H_1 is true.

In order to use the Bayes' criterion, we assume that a cost is assigned to the possible decisions. We can define $C_{ij}\left(i,j=0,1\right)$ as the cost associated with the decision D_i, when hypothesis H_j is true. In particular, the costs for this binary hypothesis test problem are C_{00} to case (1), C_{01} to case (2), C_{10} to case (3), and C_{11} to case (4). The goal in our Bayes' criterion is to determine the optimal interference range to minimize the average cost $E[C]$, also known as Bayes risk r in [29]. Denote $P\left(D_i \left| H_j\right.\right)$ as the joint probability that we decide D_i when the hypothesis H_j is true. The Bayes risk is

$$r = E[C] = \sum\nolimits_{i,j} C_{ij} P\left(D_i, H_j\right) \tag{3}$$

The cost C_{ij} may be chosen to be particular network performances. In this paper, we use the uniform cost model ($C_{00} = C_{11} = 0$ and $C_{01} = C_{10} = 1$) for simplicity. This assumption is reasonable, as there is no cost of similarity when the two models make the same decision, as in [29] and [30]. From Bayes' rule, the Bayes risk can be expressed as follows:

$$\begin{aligned} r &= P(D_0, H_1) + P(D_1, H_0) \\ &= P(H_1) + P(D_1) - 2P(H_1|D_1)\,P(D_1) \end{aligned} \tag{4}$$

where $P(H_1)$ and $P(D_1)$ are the probabilities of physical and protocol feasibility distribution, respectively. $P(H_1|D_1)$ is the conditional feasibility distribution of physical model given successfully received of the protocol model. Those feasibility distributions will be deduced in the following section.

4 Feasibility distributions

Based on the network model and according to the stochastic geometry, we provide the feasibility distributions of binomial and Poisson wireless networks.

4.1 Binomial wireless networks

Assume that M interference transmitters are independently and uniformly distributed over A. A is a circle center at the origin with radius of R. Thus, the interference transmitters are drawn from a BPP of density $\lambda = M/\left(\pi R^2\right)$. We denote the BPP by Φ_M. According to the coverage probability of [34] and the standard results in stochastic geometry [37], following three distributions can be obtained.

Lemma 1 *The feasibility distribution of the physical model under BPP is*

$$P^{BPP}(H_1) = e^{-\zeta}\left(1 + \frac{\Phi(R)}{R^2}\right)^M \tag{5}$$

where $\zeta = \beta/\mathrm{SNR}$, $\Phi(x) = \frac{2}{\beta}\Psi(x) - x^2$,
$\Psi(x) = \int_0^x \frac{t^{\alpha+1}}{1+\beta^{-1}t^{\alpha}}dt$
$= \left(\frac{x^{\alpha+2}}{\alpha+2}\right){}_2F_1\left(\left[1, \frac{2}{\alpha}+1\right]; \frac{2}{\alpha}+2, -\frac{x^{\alpha}}{\beta}\right)$,
and ${}_2F_1$ *is the Gauss hypergeometric function,*
${}_2F_1([a,b];c,x)$
$= \frac{\Gamma(c)}{\Gamma(b)\Gamma(c-b)}\int_0^1 v^{b-1}(1-v)^{c-b-1}(1-xv)^{-a}dv$,
and $\Gamma(\cdot)$ *is the gamma function.*

Proof This result follows from [34], by setting the exclusion zone radius (the area of no active interference transmitters) r_{in} to be zero and the transmitting probability (the active probability of interference transmitters) p to be one. In the physical interference model, there is no location constraint for the transmitters, and it is reasonable

to set r_{in} to be zero. For the simplicity of derivation, we set the transmitting probability to be one, as in [29] and [30]. When considering transmitting probability, the feasibility distribution can also be calculated. More complex and challenging cases with spatio-temporal traffic, where p is decided by a stochastic process, can be investigated by combining stochastic geometry and queuing theory as in [38]. □

Lemma 2 *The feasibility distribution of the protocol model under BPP is*

$$P^{BPP}(D_1) = \left(1 - \frac{R_I^2}{R^2}\right)^M \tag{6}$$

Proof According to [37], for a binomial point process with M points in a compact set A, the void probabilities of a point process are the probabilities of there being no point of the process in given test sets B:

$$P(\mathrm{N}(B) = 0) = \frac{(\nu_d(A) - \nu_d(B))^M}{\nu_d(A)^M} \tag{7}$$

where $\mathrm{N}(B)$ is the number of point in B, $\nu_d(B)$ is the volume of B.

The feasibility distribution of the protocol model under BPP, denoted by $P^{\mathrm{BPP}}(D_1)$, is the probability of there being no point of interference transmitter in the interference range of the reference receiver. The interference range in this paper is the circle centered at the reference receiver with radius R_I. Substitute the interference range for B, πR_I^2 for $\nu_d(B)$, and πR^2 for $\nu_d(A)$ achieves Lemma 2. □

Lemma 3 *The conditional feasibility distribution of physical model given successfully received of protocol model under BPP is*

$$P^{BPP}(H_1|D_1) = e^{-\zeta}\left(1 + \frac{\Phi(R) - \Phi(R_I)}{R^2}\right)^M \tag{8}$$

Proof Similar to the proof of Lemma 1, this is achieved by setting the exclusion zone radius r_{in} to be R_I and the transmitting probability p to be one. Here, we set the exclusion zone radius to be R_I, means there being no interference transmitter in the interference range. □

Other distributions, derived from H and D, are expressible in terms of $P^{\mathrm{BPP}}(H_1|D_1)$, $P^{\mathrm{BPP}}(H_1)$, and $P^{\mathrm{BPP}}(D_1)$.

4.2 Poisson wireless networks

Assume that the interference transmitters are drawn from a PPP, denoted by Φ, with density λ over A. A is a circle center at the origin with a radius of R. The number of interference transmitters M within region A is Poisson with mean $E[M] = \lambda\pi R^2$. The feasibility distributions can be obtained by taking the expectation of the three distributions in BPP with respect to M.

Lemma 4 *The feasibility distribution of the physical model under PPP is*

$$P^{PPP}(H_1) = \exp\{-\zeta + \lambda\pi\Phi(R)\} \tag{9}$$

Proof Similar to the proof of Lemma 1, this result follows from [34], by setting the exclusion zone radius r_{in} to be zero and the transmitting probability p to be one. □

Lemma 5 *The feasibility distribution of the protocol model under PPP is*

$$P^{PPP}(D_1) = \exp\left\{-\lambda\pi R_I^2\right\} \tag{10}$$

Proof From [37] we know, in a homogeneous Poisson point process with density λ, the void probabilities of a point process are the probabilities of there being no point of the process in given test sets B:

$$P(\mathrm{N}(B) = 0) = \exp\{-\lambda\nu_d(B)\} \tag{11}$$

where $\mathrm{N}(B)$ is the number of point in B, $\nu_d(B)$ is the volume of B.

The feasibility distribution of the protocol model under PPP, denoted by $P^{\mathrm{PPP}}(D_1)$, is the probability of there being no point of interference transmitter in the interference range of the reference receiver. The interference range in this paper is the circle centered at the reference receiver with radius R_I. Substitute the interference range for B, and πR_I^2 for $\nu_d(B)$ achieves Lemma 5. □

Lemma 6 *The conditional feasibility distribution of physical model given successfully reception of protocol model under PPP is*

$$\begin{aligned} P^{PPP}(H_1|D_1) = \exp\{&-\zeta + \pi\lambda\Phi(R) \\ &- \pi\lambda\Phi(R_I)\} \end{aligned} \tag{12}$$

Proof Similar to the proof of Lemma 3, this result follows from [34], by setting the exclusion zone radius r_{in} to be R_I and the transmitting probability p to be one. □

Other distributions, derived from H and D, are expressible in terms of $P^{\mathrm{PPP}}(H_1|D_1)$, $P^{\mathrm{PPP}}(H_1)$, and $P^{\mathrm{PPP}}(D_1)$.

5 Optimal interference range

Combining the binary hypothesis testing and the feasibility distributions for binomial and Poisson wireless networks, we obtain the Bayes risk for protocol interference model under the physical interference model. By studying the first derivative of the Bayes risk, we achieve the equation for optimal interference range for minimum Bayes risk in binomial and finite Poisson wireless

networks. Furthermore, the Bayes risk and optimal interference range in infinite Poisson wireless networks can be found by taking the limit of those in the finite Poisson wireless networks as $R \to \infty$.

5.1 Binomial wireless networks

Proposition 1 *The Bayes risk in binomial wireless networks, denoted by r^{BPP}, under the uniform cost model is*

$$\begin{aligned} r^{BPP} &= P^{BPP}(H_1) + P^{BPP}(D_1) \\ &\quad - 2P^{BPP}(H_1|D_1)\,P^{BPP}(D_1) \\ &= e^{-\zeta}\left(1+\frac{\Phi(R)}{R^2}\right)^M + \left(1-\frac{R_I^2}{R^2}\right)^M \\ &\quad - 2e^{-\zeta}\left(1+\frac{\Phi(R)-\Phi(R_I)}{R^2}\right)^M \\ &\quad \times \left(1-\frac{R_I^2}{R^2}\right)^M \end{aligned} \tag{13}$$

Proof The result is immediate from (4) and substituting feasibility distribution expression from (5), (6), and (8). □

Theorem 1 (Optimal interference range for minimum Bayes risk) *Under the uniform cost model, the optimal interference range for minimum Bayes risk in binomial wireless networks always exists. When $\zeta \geq \log 2$, the optimal interference range is R. This can hardly be set as interference range, as only the reference transmitter is allowed to transmit. When $\zeta < \log 2$, the optimal interference range is the unique solution to*

$$\begin{aligned} &e^{\zeta}\left(1+(\Phi(R)-\Phi(R_I))/R^2\right)^{-M} = \\ &2-\frac{2\beta R\left(R^2-R_I^2\right)}{R_I\left(\beta+R_I^{\alpha}\right)\left(R^2+\Phi(R)-\Phi(R_I)\right)} \end{aligned} \tag{14}$$

Proof The proof is in Appendix A □

5.2 Finite poisson wireless networks

Proposition 2 *The Bayes risk under finite PPP, denoted by r^{PPP}, under the uniform cost model is*

$$\begin{aligned} r^{PPP} &= P^{PPP}(H_1) + P^{PPP}(D_1) \\ &\quad - 2P^{PPP}(H_1|D_1)\,P^{PPP}(D_1) \\ &= \exp\{-\zeta+\lambda\pi\Phi(R)\} + \exp\left\{-\lambda\pi R_I^2\right\} \\ &\quad - 2\exp\{-\zeta+\lambda\pi\Phi(R) \\ &\quad - \lambda\pi\left(\Phi(R_I)+R_I^2\right)\} \end{aligned} \tag{15}$$

Proof Similar to Proposition 1 by substituting feasibility distribution expression from (9), (10), and (12). □

Theorem 2 (Optimal interference range for minimum Bayes risk) *Under the uniform cost model, the optimal interference range for minimum Bayes risk under finite PPP is the unique solution to*

$$\frac{\beta+R_I^{\alpha}}{2R_I^{\alpha}} = \exp\{-\zeta+\lambda\pi\Phi(R)-\lambda\pi\Phi(R_I)\} \tag{16}$$

The solution exists if and only if

$$\zeta < \log\left(\left(2R^{\alpha}\right)/\left(\beta+R^{\alpha}\right)\right) \tag{17}$$

Proof The proof is in Appendix B. □

5.3 Infinite poisson wireless networks

For the PPP on the entire plan, the corresponding results can be obtained from the PPP over a finite region A by taking the limit as $R \to \infty$. The results are as follows. The feasibility distributions of infinite PPP are similar to those of finite PPP by replacing $\Phi(R)$ to $\lim_{R\to\infty}\Phi(R) = -2\pi\beta^{2/\alpha}\csc(2\pi/\alpha)/\alpha\csc(2\pi/\alpha)/\alpha$.

The Bayes risk is

$$\begin{aligned} r^{\text{infPPP}} &= \exp\left\{-\zeta-2\lambda\pi^2\beta^{2/\alpha}\csc(2\pi/\alpha)/\alpha\csc(2\pi/\alpha)/\alpha\right\} \\ &\quad + \exp\left\{-\lambda\pi R_I^2\right\} - 2\exp\{-\zeta \\ &\quad - 2\lambda\pi^2\beta^{2/\alpha}\csc(2\pi/\alpha)/\alpha \\ &\quad - \lambda\pi\left(\Phi(R_I)+R_I^2\right)\} \end{aligned} \tag{18}$$

Corollary 1 (Optimal interference range for minimum Bayes risk) *Under the uniform cost model, the optimal interference range for minimum Bayes risk under infinite PPP is the unique solution to*

$$\begin{aligned} \frac{\beta+R_I^{\alpha}}{2R_I^{\alpha}} &= \exp\{-\zeta-2\lambda\pi^2\beta^{2/\alpha}\csc(2\pi/\alpha)/\alpha \\ &\quad - \lambda\pi\Phi(R_I)\} \end{aligned} \tag{19}$$

The solution exists if and only if

$$\zeta < \log 2 \tag{20}$$

Proof This result follows from Theorem 2 by taking the limit as $R \to \infty$. □

Corollary 2 *For two dimension networks, when the reference transmitter is at unit distance from the receiver and uniform cost model is adopted, the Bayes risk and the optimal interference range under infinite PPP are the same with those in* [30].

Proof The proof is in Appendix C. □

6 Numerical results

In our simulation, we use the similar environment parameters of [30]. Notice that distance is normalized to the distance from TX_0 to RX_0, and the transmitter density is one hundred times of that in [30]. Numerical results for Bayes risk, optimal interference range, receiver operating characteristic (ROC), and area under curve (AUC) for both BPP and PPP are shown as follows. The proposed methods can be adopted to achieve the interference range for wireless networks. We utilize the ROC and AUC to evaluate the performance of each method. The ROC is used to show the tradeoff between type I (false rejection $P_I = P(D_1|H_0)$) and type II (false acceptance $P_{II} = P(D_0|H_1)$) error rates. The AUC is the area under the ROC curve and is a useful numerical value to evaluate the performance of the proposed method.

6.1 Bayes risks and first derivatives

The Bayes risks and the first derivatives under BPP, finite PPP, and infinite PPP are shown in Fig 1. In order to show the difference of the three point processes, we set the area to be a disk of radius $R = 10$. When the area is sufficiently large, the results of BPP and finite PPP converge to those of infinite PPP. The density of interference transmitter is $\lambda = 2 \times 10^{-2}$. The path loss exponent is $\alpha = 3$. The SINR threshold is $\beta = 5$. We first investigate the case without noise, where the power of background noise is set to be 0, and the SNR is infinite, i.e., SNR $= +\infty$.

Figure 1a shows the Bayes risks decrease firstly then increase with the increment of the interference range. The minimum Bayes risks are achieved at the optimal interference range. From the numerical results, we know that there is a unique optimal interference range which can minimize the Bayes risk for BPP, finite PPP, and infinite PPP, respectively. For BPP, the optimal interference range is $R_I^{\mathrm{BPP}} = 2.00$. For finite PPP, the optimal interference range is $R_I^{\mathrm{PPP}} = 2.02$. For infinite BPP, the optimal interference range is $R_I^{\mathrm{inf\,PPP}} = 2.11$. This indicates the BPP has the smallest optimal range, which allows more transmitters to be active simultaneously. Besides, with small interference range, the Bayes risk of BPP is almost the same as the Bayes risk of finite PPP, and obviously smaller than that of infinite PPP. This means, for finite networks with small interference range, using the infinite PPP method will overestimate the Bayes risk.

As shown in Fig 1b, with the growth of interference range, the first derivatives turn from negative to positive. For $0 < R_I < 10$, there is a unique zero point, which acts as the optimal interference range, for the BPP, finite PPP, and infinite PPP, respectively. It can be found that the first derivative of the BPP is the first to reach the zero point, and follows the first derivative of the finite PPP, and the last is the first derivative of the infinite PPP.

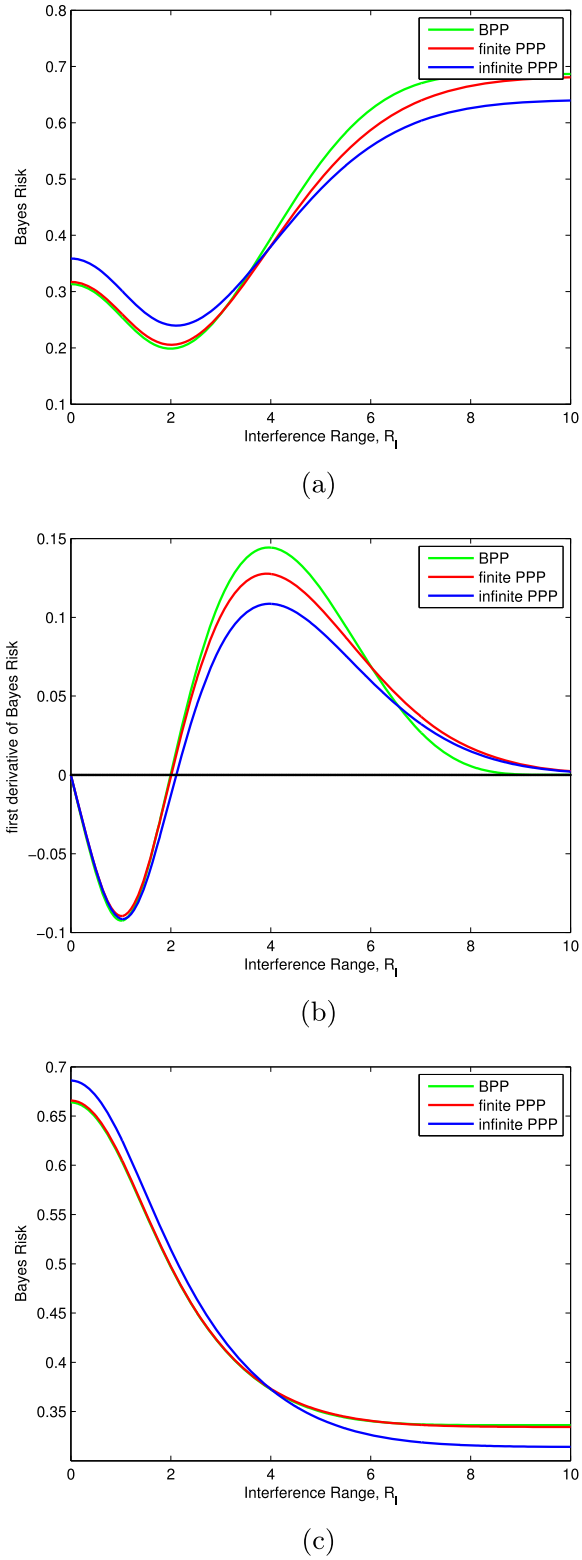

Fig. 1 Bayes risks and the first derivatives under BPP, finite PPP, and infinite PPP. **a** Bayes risks (SNR = + ∞). **b** The first derivatives of Bayes risks. **c** Bayes risks (SNR = 7)

When SNR is sufficiently large $\left(\text{SNR} > \frac{\beta}{\log 2}\right)$, similar results can be achieved. For the case with large noise $\left(\text{SNR} \leq \frac{\beta}{\log 2}\right)$, we set SNR = 7 as an example in Fig 1c. It is obvious that the Bayes risks are monotonously decreasing, and the optimal interference ranges for the minimum Bayes risks are at the maximum network radius R. This indicates that only the reference transmitter can be active, which is inefficiency for a practical network. Consequently, the Bayes methods cannot be directly applied to the network with heavy noise, and more effort should be taken in this aspect.

6.2 Parameters influence the optimal interference range

Figure 2 shows the optimal interference range influenced by parameters (λ, β, α), under BPP, finite PPP, and infinite PPP. The area is a disk of radius $R = 10$. The power of background noise is set to be 0, and the SNR is infinite, i.e., SNR $= +\infty$.

Figure 2a shows the optimal interference ranges increase with the density λ growing from 2×10^{-3} to 2×10^{-1}. The settings of other parameters are $\alpha = 3$ and $\beta = 5$. This is quite hard to understand. As the physical feasibility decreases with λ, in order to minimize the Bayes risks, the protocol feasibility must likewise be decreased by increasing R_I or λ. Notice that, in order to minimize the Bayes risks, only increasing λ is not enough, and it must be additionally increased by expanding R_I. It is quite obvious that the optimal interference range of BPP and finite PPP are smaller than that of infinite PPP. As in infinite PPP, the network radius is infinite, which leads to more interference compared with BPP and finite PPP. In order to minimize the risk, a relatively larger interference range is needed for infinite PPP. Besides, the optimal interference range of BPP is slightly lower than that of finite PPP.

Figure 2b shows the optimal interference ranges increase with the SINR threshold β growing from 0.5 to 50. The settings of other parameters are $\lambda = 2 \times 10^{-2}$ and $\alpha = 3$. This is because the physical feasibility decreases with SINR threshold β, and the protocol model feasibility must be decreased by increasing R_I. Similar to Fig. 2a, the optimal interference range of BPP and finite PPP are smaller than that of infinite PPP, and the optimal interference range of BPP is slightly lower than that of finite PPP.

Figure 2c shows the optimal interference ranges decrease with the path loss exponent α growing from 2 to 8. The settings of other parameters are $\lambda = 2 \times 10^{-2}$ and $\beta = 5$. Bigger path loss exponent means higher power attenuation, which leads to lower interference and higher protocol feasibility. In order to minimize the Bayes risks, the protocol feasibility must likewise be increased by decreasing R_I. Again,

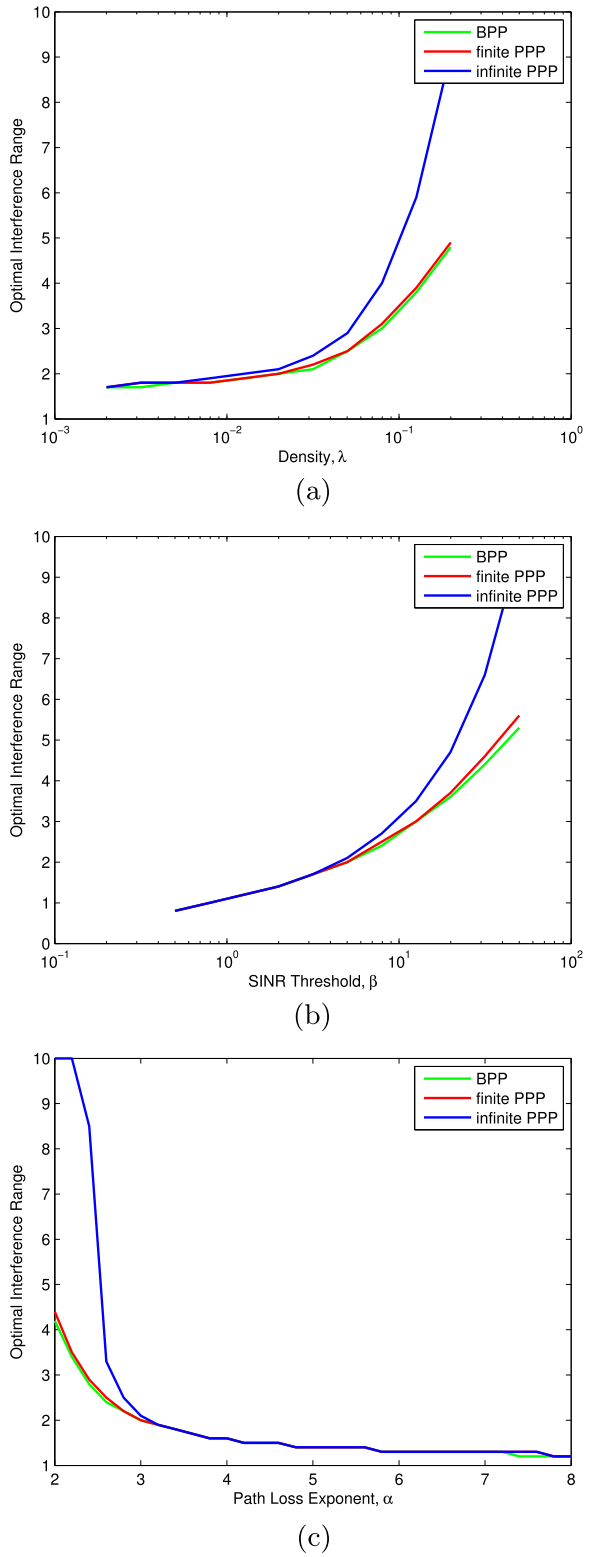

Fig. 2 Optimal interference range influenced by parameters. **a** Optimal interference range vs. densityλ. **b** Optimal interference range vs. SINR threshold β. **c** Optimal interference range vs. path loss exponent α

the optimal interference range of BPP and finite PPP are smaller than that of infinite PPP, and the optimal interference range of BPP is slightly lower than that of finite PPP.

Those simulation results indicate the optimal interference range should be appropriately chosen according to the network parameters. The casual setting of the interference range will raise the Bayes risk and depress the performance of wireless networks.

6.3 ROC and AUC compare

Figure 3 compares the ROC and AUC of BPP, finite PPP, and infinite PPP. The path loss exponent is $\alpha = 3$. The SINR threshold is β =5 and SNR $= +\infty$. Figure 3a shows the ROC curves travel from bottom-right to top-left, as the interference range R_I grows. The network radius is $R = 10$. The density of interference transmitter is $\lambda = 2 \times 10^{-2}$. The ROC of BPP is in the lowest place and close to the ROC of finite PPP. It is obvious that the ROC of both BPP and finite PPP is under that of infinite PPP, which means the BPP and finite PPP methods have a lower error rate than the infinite PPP method. That is to say, the BPP method and the finite PPP methods perform better in the finite networks. Figure 3b shows the AUC of BPP, finite PPP, and infinite PPP vary with the different network radiuses. The network radiuses range from 10 to 200, and the density of interference transmitter is set to be $\lambda = 2 \times 10^{-2}$, $\lambda = 1 \times 10^{-1}$, and $\lambda = 3 \times 10^{-1}$. From the simulation results, we know the AUC of BPP and finite PPP is smaller than the AUC of infinite PPP when the network radius is small. With a larger network radius, those AUCs are nearly the same. Those results indicate that the BPP method and the finite PPP method have better performance in small networks and have similar performance to infinite PPP in large networks. Furthermore, when $\lambda = 1 \times 10^{-1}$ and $\lambda = 3 \times 10^{-1}$, there is an obvious advantage of the BPP method over the finite PPP method. That is to say, the BPP method performs better than the PPP methods in small networks with high node density. When $\lambda = 2 \times 10^{-2}$, the AUC of finite PPP and infinite PPP are nearly the same. This implies that the two PPP methods have the same performance in wireless networks with large density.

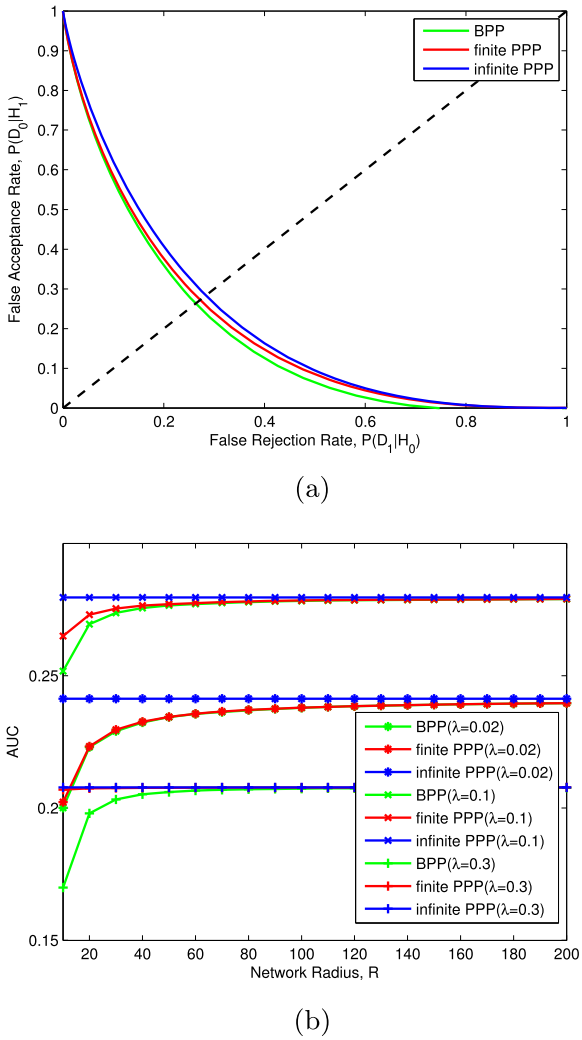

Fig. 3 ROC and AUC compare. **a** ROC for BPP, finite PPP, and infinite PPP. **b** AUC for BPP, finite PPP, and infinite PPP

7 Conclusion

In this paper, we provide methods to achieve the optimal interference range for minimum Bayes risk, under the assumptions of both binomial and Poisson wireless networks. For Poisson wireless networks, both finite and infinite networks are concerned. Following that, several numerical results are provided. Simulation results show that in the finite wireless network, the BPP method performs better than the PPP methods. The analytical and numerical results may assist in the more accurate and effective use of the protocol interference model.

In future work, it is of interest to relate the risk with what a user of networks may care, e.g., throughput, delay, and reliability. This may directly indicate the effect of interference range setting on the network performance. Additionally, networks with medium access control (MAC) protocol (e.g., ALOHA and CSMA), unsaturated traffic(e.g., spatio-temporal traffic), and more fading factors (e.g., Rician and Nakagami) need further studied.

Appendix

Appendix A

Proof of theorem 1

Proof The first derivative of r^{BPP} to interference range R_I is

$$\begin{aligned}\frac{dr^{\mathrm{BPP}}}{dR_I} &= M\left(1-\frac{R_I^2}{R^2}\right)^{M-1}\left(-\frac{2R_I}{R^2}\right)\\ &- 2e^{-\zeta}\left(1-\frac{R_I^2}{R^2}\right)^{M-1}\\ &\times\left(1+\frac{\Phi(R)-\Phi(R_I)}{R^2}\right)^{M-1}\\ &\times\left(M\left(\frac{2\beta R_I}{R^2\left(\beta+R_I^{\alpha}\right)}\right)\left(1-\frac{R_I^2}{R^2}\right)\right.\\ &+\left.\left(1+\frac{\Phi(R)-\Phi(R_I)}{R^2}\right)M\left(\frac{-2R_I}{R^2}\right)\right)\\ &= M\left(1-\frac{R_I^2}{R^2}\right)^{M-1}\left(-\frac{2R_I}{R^2}\right)\\ &\times e^{-\zeta}\left(1+\frac{\Phi(R)-\Phi(R_I)}{R^2}\right)^{M}\\ &\times\left(e^{\zeta}\left(1+\frac{\Phi(R)-\Phi(R_I)}{R^2}\right)^{-M}-2\right.\\ &+\left.\frac{2\beta\left(R^2-R_I^2\right)}{\left(\beta+R_I^{\alpha}\right)\left(R^2+\Phi(R)-\Phi(R_I)\right)}\right)\end{aligned}\tag{21}$$

In order to analyze the first derivative, the following two functions are defined.

$$\begin{aligned}f_1 &= e^{\zeta}\left(1+\left(\Phi(R)-\Phi(R_I)\right)/R^2\right)^{-M}\\ f_2 &= 2-\frac{2\beta\left(R^2-R_I^2\right)}{\left(\beta+R_I^{\alpha}\right)\left(R^2+\Phi(R)-\Phi(R_I)\right)}\end{aligned}\tag{22}$$

The first derivative of r^{BPP} to interference range R_I can be expressed as follows:

$$\frac{dr^{\mathrm{BPP}}}{dR_I} = g_1(R_I)\left(f_1-f_2\right)\tag{23}$$

where $g_1(R_I) = Me^{-\zeta}\left(-\frac{2R_I}{R^2}\right)\left(1-\frac{R_I^2}{R^2}\right)^{M-1}h(R_I)$, and $h(R_I) = \left(1+\frac{\Phi(R)-\Phi(R_I)}{R^2}\right)^{M}$. It is easy to know that $g_1(R_I) < 0$ for all R_I, as $h(R_I) > 0$ ($\Phi(x)$ is monotonous decreasing). The monotonicity of r^{BPP} can be easily decided by analyzing $f_1 - f_2$.

For $1/f_1$, the first derivative is

$$\begin{aligned}\left(1/f_1\right)' &= Me^{-\zeta}\left(1+\frac{\Phi(R)-\Phi(R_I)}{R^2}\right)^{M-1}\\ &\times\left(\frac{2\beta R_I}{R^2\left(\beta+R_I^{\alpha}\right)}\right)\\ &\geq 0\end{aligned}\tag{24}$$

From (24), we know $1/f_1$ is monotonously increasing, and f_1 is monotonously decreasing. The limiting values are $\lim_{R_I\to 0} f_1 = e^{\zeta}\left(1+\Phi(R)/R^2\right)^{-M}$, and $\lim_{R_I\to R} f_1 = e^{\zeta}$.

For f_2, the first derivative is

$$\begin{aligned}f_2' &= \left(\left(\beta+R_I^{\alpha}\right)\left(R^2+\Phi(R)-\Phi(R_I)\right)\right)^{-2}\\ &\times\left(4\beta R_I\left(\beta+R_I^{\alpha}\right)\left(R^2+\Phi(R)-\Phi(R_I)\right)\right.\\ &+\left.2\beta\left(R^2-R_I^2\right)\left(\alpha R_I^{\alpha-1}\left(R^2+\Phi(R)\right.\right.\right.\\ &-\left.\left.\left.\Phi(R_I)\right)+2\beta R_I\right)\right)\\ &\geq 0\end{aligned}\tag{25}$$

From (25), we know f_2 is monotonously increasing, and the limiting values are $\lim_{R_I\to 0} f_2 = 2-2R^2/\left(R^2-\Phi(R)\right)$ and $\lim_{R_I\to R} f_2 = 2$.

In summary, f_1 is decreasing from $e^{\zeta}\left(1+\frac{\Phi(R)}{R^2}\right)^{-M}$ down to e^{ζ}, and f_2 is increasing from $2-\frac{2R^2}{R^2-\Phi(R)}$ up to 2. It is clear that f_1 and f_2 have a unique intersection, which minimizes the Bayes risk, if and only if $e^{\zeta} < 2$, i.e., $\zeta < \log 2$. That is to say, when $\zeta < \log 2$, the optimal interference range is achieved at $f_1 = f_2$. Denote the point $f_1 = f_2$ by R_I^{BPP}. When $R_I < R_I^{\mathrm{BPP}}$, $f_1 > f_2$, $\frac{dr^{\mathrm{BPP}}}{dR_I} < 0$, and r^{BPP} is monotonously decreasing. When $R_I > R_I^{\mathrm{BPP}}$, $f_1 < f_2$, $\frac{dr^{\mathrm{BPP}}}{dR_I} > 0$, and r^{BPP} is monotonously increasing. As a consequence, the minimum Bayes risk r^{BPP} is achieved at R_I^{BPP}, which is the optimal interference range of BPP. If $\zeta \geq \log 2$, f_1 will always be bigger than f_2, and $\frac{dr^{\mathrm{BPP}}}{dR_I} \leq 0$ is tenable for all $R_I \in [0, R]$. Under this situation, the optimal interference range for minimum r^{BPP} is R. □

Appendix B

Proof of theorem 2

Proof The first derivative of r^{PPP} to interference range R_I is

$$\begin{aligned}\frac{dr^{\mathrm{PPP}}}{dR_I} &= \exp\left\{-\lambda\pi R_I^2\right\}\left(-2\lambda\pi R_I\right)\\ &- 2\exp\left\{-c-\lambda\pi\left(\Phi(R_I)+R_I^2\right)\right\}\\ &\times\left(\frac{-2\lambda\pi R_I^{\alpha+1}}{\beta+R_I^{\alpha}}\right)\\ &= \exp\left\{-\lambda\pi R_I^2\right\}\left(\frac{-4\lambda\pi R_I^{\alpha+1}}{\beta+R_I^{\alpha}}\right)\\ &\times\left(\frac{\beta+R_I^{\alpha}}{2R_I^{\alpha}}-\exp\left\{-c-\lambda\pi\Phi(R_I)\right\}\right)\end{aligned}\tag{26}$$

where $c = \zeta - \lambda\pi\Phi(R)$ is a variable that irrelevant to R_I. Similar to the Appendix A, we define the following two functions to analyze the derivative.

$$\begin{aligned}f_3 &= \frac{\beta+R_I^{\alpha}}{2R_I^{\alpha}}\\ f_4 &= \exp\left\{-c-\lambda\pi\Phi(R_I)\right\}\end{aligned}\tag{27}$$

The first derivative of r^{PPP} to interference range R_I can be expressed as follows:

$$\frac{dr^{\mathrm{PPP}}}{dR_I} = g_2(R_I)\left(f_3 - f_4\right) \tag{28}$$

where $g_2(R_I) = \exp\left\{-\lambda\pi R_I^2\right\}\left(\frac{-4\lambda\pi R_I^{\alpha+1}}{\beta+R_I^{\alpha}}\right) < 0$, for all R_I. The monotonicity of r^{PPP} can be easily decided by analyzing $f_3 - f_4$.

For f_3, the first derivative is

$$f_3{}' = \frac{-\alpha\beta}{R_I^{\alpha+1}} < 0 \tag{29}$$

From (29), we know f_3 is monotonously decreasing, and the limiting values are $\lim_{R_I\to 0} f_3 = +\infty$ and $\lim_{R_I\to R} f_3 = \frac{\beta+R^{\alpha}}{2R^{\alpha}}$.

For f_4, the first derivative is

$$f_4{}' = \exp\left\{-c - \lambda\pi\Phi(R_I)\right\}\left(\frac{2\lambda\pi\beta R_I}{\beta + R_I^{\alpha}}\right) \geq 0 \tag{30}$$

From (30), we know f_4 is monotonously increasing, and the limiting values are $\lim_{R_I\to 0} f_4 = e^{-c}$ and $\lim_{R_I\to R} f_4 = \exp\left\{-c - \lambda\pi\Phi(R)\right\} = e^{-\zeta}$.

In summary, f_3 is decreasing from $+\infty$ down to $(\beta + R^{\alpha})/(2R^{\alpha})$, and f_4 is increasing from e^{-c} up to $e^{-\zeta}$. It is clear that f_3 and f_4 have a unique intersection, which minimizes the Bayes risk, if and only if $\zeta < \log\left((2R^{\alpha})/(\beta + R^{\alpha})\right)$. That is to say, when $\zeta < \log\left((2R^{\alpha})/(\beta + R^{\alpha})\right)$, the optimal interference range is achieved at $f_3 = f_4$. Denote the point $f_3 = f_4$ by R_I^{PPP}. When $R_I < R_I^{\mathrm{PPP}}$, $f_3 > f_4$, $\frac{dr^{\mathrm{PPP}}}{dR_I} < 0$, and r^{PPP} is monotonously decreasing. When $R_I > R_I^{\mathrm{PPP}}$, $f_3 < f_4$, $\frac{dr^{\mathrm{PPP}}}{dR_I} > 0$, and r^{PPP} is monotonously increasing. As a consequence, the minimum Bayes risk r^{PPP} is achieved at R_I^{PPP}, which is the optimal interference range of PPP. If $\zeta \geq \log\left((2R^{\alpha})(\beta + R^{\alpha})\right)$, f_3 will always be bigger than f_4, and $\frac{dr^{\mathrm{PPP}}}{dR_I} \leq 0$ is tenable for all $R_I \in [0, R]$. Under this situation, the optimal interference range for minimum r^{PPP} is R. □

Appendix C

Proof of corollary 2

Proof We show the coincidence of the Bayes risk and the optimal interference range in turn.

Bayes risk

For two dimension network, when the reference transmitter is at unit distance from the receiver and uniform cost model are adopted, the Bayes risk in [30] is

$$\begin{aligned} r^{\mathrm{infPPP}} &= \exp\left\{-2\lambda\pi^2\beta^{2/\alpha}\csc(2\pi/\alpha)/\alpha\right\} \\ &+ \exp\left\{-\lambda\pi R_I^2\right\} \\ &- 2\exp\left\{-2\lambda\pi^2\beta^{2/\alpha}\csc(2\pi/\alpha)/\alpha\right. \\ &- \left.\zeta - \lambda\pi\beta^{2/\alpha} I\left(R_I^{\alpha}/\beta, 2/\alpha\right)\right\} \end{aligned} \tag{31}$$

where $I(u, v) = v\int_0^u t^v/(1+t)dt$.

This is achieved from [30] by letting $n = 2$, $r_t = 1$, $r_0 = R_I$, $\eta = 1/\mathrm{SNR}$, $c_{01} = c_{10} = 1$, and $c_{00} = c_{11} = 0$. The only different between (31) and (18) is the last part of the third exponent. To prove the coincidence of (31) and (18), we only have to demonstrate $\beta^{2/\alpha} I\left(R_I^{\alpha}/\beta, 2/\alpha\right) = \Phi(R_I) + R_I^2$. The proof is as follow:

$$\begin{aligned} \beta^{2/\alpha} I\left(\frac{R_I^{\alpha}}{\beta}, \frac{2}{\alpha}\right) &= \beta^{2/\alpha}\frac{2}{\alpha}\int_0^{R_I^{\alpha}/\beta} \frac{t^{2/\alpha}}{1+t}dt \\ &= \beta^{2/\alpha}\frac{2}{\alpha}\int_0^{R_I} \frac{\left(\beta^{-1}u^{\alpha}\right)^{2/\alpha}}{1+\beta^{-1}u^{\alpha}} \\ &\times \left(\frac{\alpha}{\beta}\right)u^{\alpha-1}du \\ &= \frac{2}{\beta}\int_0^{R_I} \frac{u^{\alpha+1}}{1+\beta^{-1}u^{\alpha}}du \\ &= \Phi(R_I) + R_I^2 \end{aligned} \tag{32}$$

Optimal interference range

For two dimension network, when the reference transmitter is at unit distance from the receiver and uniform cost model are adopted, the optimal interference range in [30] is the unique solution to

$$\begin{aligned} \frac{1}{2}\left(1 + \frac{\beta}{R_I^{\alpha}}\right) &= \exp\left\{-2\lambda\pi^2\beta^{2/\alpha}\csc(2\pi/\alpha)/\alpha\right. \\ &- \zeta + \lambda\pi R_I^2 \\ &- \left.\lambda\pi\beta^{2/\alpha} I\left(R_I^{\alpha}/\beta, 2/\alpha\right)\right\} \end{aligned} \tag{33}$$

This solution exists if and only if

$$\zeta < \log 2 \tag{34}$$

This is achieved from [30] by letting $n = 2$, $r_T = 1$, $r_O = R_I$, $\zeta = 1/\mathrm{SNR}$, $c_{01} = c_{10} = 1$, and $c_{00} = c_{11} = 0$. Recalling (32), we can easily prove the right hand side of (33) coincides with that of (19). The equality of the left hand sides is obvious. The condition that optimal interference range exists (34) is the same as (20). □

Abbreviations

AUC: Area under curve; BPP: Binomial point process; i.i.d.: Independent and identically distributed; PPP: Poisson point process; PRK: Physical-ratio-K; ROC: Receiver operating characteristic; SINR: Signal-to-interference-and-noise ratio; SNR: Average signal-to-noise ratio

Acknowledgements

The authors wish to acknowledge the helpful comments of the Associate Editor and the anonymous reviewers.

Authors' contributions
All authors contribute to the concept, design, and developments of the theory analysis and the simulation results in this manuscript. All authors read and approved the final manuscript.

Authors' information
Min Ouyang received his B.S. degree in Communication Engineering from Jilin University, China, in 2014. He is currently working toward the Ph.D. degree in Communication Engineering in the same university by postgraduate recommendation. He has been devoted to researching on capacity analysis for wireless networks. His current research interests include capacity analysis and stochastic geometry modeling in wireless networks.
Wenxiao Shi received the B.S. degree in Communication Engineering from Changchun Institute of Posts and Telecommunications, China, in 1983; the M.S. degree in Electrical Engineering from Harbin Institute of Technology, China, in 1991; and the Ph.D. degree in Communication and Information Systems from Jilin University, China, in 2006. He is a Professor in the College of Communication Engineering, Jilin University, China, since 2000. His research interests include radio resource management, access control and load balance of heterogeneous wireless networks, wireless mesh networks, free-space optical communication, mobile edge computing, etc.

Funding
This work was supported in part by the National Science Foundation of Jilin Province of China (No.20180101045JC) and in part by the National Natural Science Foundation of China (No.61373124)

Availability of data and materials
Not applicable.

Competing interests
The authors declare that they have no competing interests.

Received: 11 June 2019 Accepted: 24 October 2019
Published online: 06 November 2019

References

1. P. Gupta, P. R. Kumar, The capacity of wireless networks. IEEE Trans. Inf. Theory. **46**(2), 388–404 (2000)
2. K. Shih, Y. Chen, C. Chang, A physical/virtual carrier-sense-based power control mac protocol for collision avoidance in wireless ad hoc networks. IEEE Trans. Parallel Distrib. Syst. **22**(2), 193–207 (2011)
3. W. Ren, Q. Zhao, A. Swami, Connectivity of heterogeneous wireless networks. IEEE Trans. Inf. Theory. **57**(7), 4315–4332 (2012)
4. A. Argyriou, Cross-layer and cooperative opportunistic network coding in wireless ad hoc networks. IEEE Trans. Veh. Commun. **59**(2), 803–812 (2010)
5. X. Li, P. Kong, K. Chua, Tcp performance in ieee 802.11-based ad hoc networks with multiple wireless lossy links. IEEE. Trans. Mob. Comput. **6**(12), 1329–1342 (2007)
6. J. Wang, W. Shi, K. Cui, F. Jin, Y. Li, Partially overlapped channel assignment for multi-channel multi-radio wireless mesh networks. EURASIP J. Wirel. Commun. Netw. **25**, 1–12 (2015)
7. Y. Ding, Y. Huang, G. Zeng, L. Xiao, Using partially overlapping channels to improve throughput in wireless mesh networks. IEEE. Trans. Mob. Comput. **11**(11), 1720–1733 (2012)
8. J. Wang, W. Shi, Y. Xu, F. Jin, Uniform description of interference and load based routing metric for wireless mesh networks. EURASIP J. Wirel. Commun. Netw. **132**, 1–11 (2014)
9. H. Ma, R. Vijayakumar, S. Roy, J. Zhu, Optimizing 802.11 wireless mesh networks based on physical carrier sensing. IEEE-ACM Trans. Netw. **17**(5), 1550–1563 (2009)
10. Y. Feng, M. Li, M. Wu, A weighted interference estimation scheme for interface switching wireless mesh networks. Wirel. Commun. Mob. Comput. **9**, 773–784 (2009)
11. R. Kapelko, On the maximum movement to the power of random sensors for coverage and interference. Pervasive Mob. Comput. **51**, 174–192 (2018)
12. G. Zhou, T. He, J. A. Stankovic, T. Abdelzaher, in *IEEE INFOCOM 2005. The Conference on Computer Communications - 24th Annual Joint Conference of the IEEE Computer and Communications Societies: 13-17 March 2005; Miami, FL, United States*. Rid: radio interference detection in wireless sensor networks (IEEE, Miami, 2005), pp. 891–901. https://doi.org/10.1109/INFCOM.2005.1498319
13. N. Lee, S. Bahk, in *COMSWARE 2007. Proceedings of the 2007 2nd International Conference on Communication System Software and Middleware and Workshops: 7-12 January 2007; Bangalore, India*. Channel allocation considering the interference range in multi-cell ofdma downlink systems, (2007), pp. 1–6. https://doi.org/10.1109/comswa.2007.382616
14. N. Lee, S. Bahk, in *WCNC 2007. 2007 IEEE Wireless Communications and Networking Conference: 11-15 March 2007; Kowloon, China*. Dynamic channel allocation using the interference range in multi-cell downlink systems, (2007), pp. 1716–1721. https://doi.org/10.1109/wcnc.2007.323
15. M. Zhou, H. Harada, P. Kong, J. S. Pathmasuntharama, in *WCNC 2010.2010 IEEE Wireless Communications and Networking Conference: 18-21 April 2010; Sydney, NSW, Australia*. Interference range analysis and scheduling among three-hop neighborhood in maritime wimax mesh networks, (2010), pp. 1–6. https://doi.org/10.1109/wcnc.2010.5506227
16. K. Lee, P. Mitchell, D. Grace, Energy efficient distributed reservation multiple access with adaptive switching requests for wireless networks. IEEE Trans. Wirel. Commun. **13**(1), 259–267 (2014)
17. C. Sum, M. A. Rahman, L. Lu, F. Kojima, H. Harada, in *WCNC 2012. 2012 IEEE Wireless Communications and Networking Conference: 1-4 April 2010; Paris, France*. On communication and interference range of IEEE 802.15.4g smart utility networks, (2012), pp. 1169–1174. https://doi.org/10.1109/wcnc.2012.6213953
18. S. Xu, T. Saadawi, Does the ieee 802.11 mac protocol work well in multihop wireless ad hoc networks?. IEEE Commun. Mag. **39**(6), 130–137 (2001)
19. K. Xu, M. Gerla, S. Bae, in *GLOBECOM'02. IEEE Global Telecommunications Conference: 17-21 November 2002; Taipei, Taiwan, China*. How effective is the ieee 802.11 rts/cts handshake in ad hoc networks, (2002), pp. 72–76. https://doi.org/10.1109/glocom.2002.1188044
20. S. Wang, V. Venkateswaran, X. Zhang, Fundamental analysis of full-duplex gains in wireless networks. IEEE-ACM Trans. Netw. **25**(3), 1401–1416 (2017)
21. J. YAO, W. Lou, C. Yang, K. Wu, Efficient interference-aware power control for wireless networks. Comput. Netw. **136**, 68–79 (2018)
22. J. YAO, W. Lou, C. Yang, K. Wu, in *ICC 2017. 2017 IEEE International Conference on Communications: 21-25 May 2017; Paris, France*. Efficient interference-aware power control in wireless ad hoc networks, (2017), pp. 1–6. https://doi.org/10.1109/icc.2017.7997363
23. K. Park, J. Choi, J. C. Hou, Y. Hu, H. Lim, Optimal physical carrier sense in wireless networks. Ad Hoc Netw. **9**(1), 16–27 (2011)
24. Y. Shi, Y. T. Hou, J. Liu, S. Kompella, Bridging the gap between protocol and physical models for wireless networks. IEEE. Trans. Mob. Comput. **12**(7), 1404–1416 (2013)
25. A. Hasan, J. G. Andrews, The guard zone in wireless ad hoc networks. IEEE Trans. Wirel. Commun. **6**(3), 897–906 (2007)
26. A. Iyer, C. Rosenberg, A. Karnik, What is the right model for wireless channel interference?. IEEE Trans. Wirel. Commun. **8**(5), 2662–2671 (2009)
27. H. Zhang, X. Che, X. Liu, X. Ju, Adaptive instantiation of the protocol interference model in wireless networked sensing and control. ACM Trans. Sensor Netw. **10**(2), 1–48 (2014)
28. A. Hasan, A. Ali, Guard zone-based scheduling in ad hoc networks. Comput. Commun. **56**, 89–97 (2015)
29. J. Wildman, S. Weber, in *WiOpt 2016. 14th International Symposium on Modeling and Optimization in Mobile, Ad Hoc, and Wireless Networks: 9-13 May 2016; Tempe, AZ, United States*. Minimizing the bayes risk of the protocol interference model in wireless poisson networks, (2016), pp. 1–8. https://doi.org/10.1109/wiopt.2016.7492923
30. J. Wildman, S. Weber, On protocol and physical interference models in poisson wireless networks. IEEE Trans. Wirel. Commun. **17**(2), 808–821 (2018)
31. Y. Zhong, X. Ge, H. H. Yang, T. Han, Q. Li, Traffic matching in 5g ultra-dense networks. IEEE Commun. Mag. **56**(8), 100–105 (2018)
32. X. Liu, Closed-form coverage probability in cellular networks with poisson point process. IEEE Trans. Veh. Technol. **68**(8), 8206–8209 (2019)
33. M. Salehi, H. Tabassum, E. Hossain, Accuracy of distance-based ranking of users in the analysis of noma systems. IEEE Trans. Commun. **67**(7), 5069–5083 (2019)

34. M. C. Valenti, D. Torrieri, S. Talarico, A direct approach to computing spatially averaged outage probability. IEEE Commun. Lett. **18**(7), 1103–1106 (2014)
35. P. Cardieri, Modeling interference in wireless ad hoc networks. IEEE Commun. Surveys Tuts. **12**(4), 551–572 (2010)
36. M. Barkat, *Signal Detection and Estimation*. (Artech House, London, 2005)
37. S. N. Chiu, D. Stoyan, W. S. Hendall, J. Mecke, *Stochastic Geometry and Its Applications*. (John Wiley Sons Ltd, Chichester, 2013)
38. Y. Zhong, G. Wang, T. Han, M. Wu, X. Ge, Qoe and cost for wireless networks with mobility under spatio-temporal traffic. IEEE ACCESS. **7**(1), 47206–47220 (2019)

Publisher's Note